Dalton Transactions

ROYAL SOCIETY OF CHEMISTRY

PAPER

View Article Online
View Journal | View Issue

Check for updates

Cite this: *Dalton Trans.*, 2020, **49**, 9495

Cooperative N–H bond activation by amido-Ge(II) cations†

Xueer Zhou,[a] Petra Vasko,[a,b] Jamie Hicks,[a] M. Ángeles Fuentes,[a] Andreas Heilmann,[a] Eugene L. Kolychev[a] and Simon Aldridge *[a]

Received 1st June 2020,
Accepted 24th June 2020

DOI: 10.1039/d0dt01960g

rsc.li/dalton

N-heterocyclic carbene (NHC) and tertiary phosphine-stabilized germylium-ylidene cations, $[R(L)Ge:]^+$, featuring tethered amido substituents at R have been synthesized *via* halide abstraction. Characterization in the solid state by X-ray crystallography shows these systems to be monomeric, featuring a two-coordinate C,N- or P,N-ligated germanium atom. The presence of the strongly Lewis acidic cationic germanium centre and proximal amide function allows for facile cleavage of N–H bonds in 1,2-fashion: the products resulting from reactions with carbazole feature a tethered secondary amine donor bound to a three-coordinate carbazolyl-Ge^{II} centre. In each case, addition of the components of the N–H bond occurs to the same face of the germanium amide function, consistent with a coordination/proton migration mechanism. Such as sequence is compatible with the idea that substrate coordination *via* the pπ orbital at germanium reduces the extent of N-to-Ge π donation from the amide, thereby enhancing the basicity of the proximal N-group.

Introduction

The metal-mediated activation of N–H bonds (particularly those in ammonia) is a challenging fundamental chemical step with potential significance to a number of important transformations of industrial relevance.[1] The scarcity of transition metal systems capable of effecting N–H cleavage *via* oxidative addition, in a manner familiar for a plethora of other E–H bonds, reflects the competing tendency of ammonia to form classical Werner complexes at unsaturated metal centres.[2]

Within p-block chemistry, a number of systems have been reported in the last 15 years which will cleave ammonia to give a derivative containing the $E(H)(NH_2)$ function,[3,4] including several carbene and related heavier group 14 species in the +2 oxidation state.[3] The presence of a low-lying formally vacant pπ orbital in such systems allows for simple coordination of amines (akin to d-block metal complexes); facile N-to-E proton transfer, however, has been proposed to offer a route to generate an amido hydride species without the need for amine dissociation.[3e,h,5,6] Moreover, in addition to single site N–H oxidative addition, heavier group 14 analogues of carbenes have also been shown to offer a number of alternative (cooperative) pathways for N–H cleavage involving H-atom transfer to a ligand site (Scheme 1). The relative propensity for different modes of activation has been shown to reflect the identity of the group 14 element/supporting ligand set (and the associated E^{II}/E^{IV} redox potential). In the case of germylene systems, for example, both single site (1,1 addition) and ligand-assisted 1,4 activation modes have been reported, depending not only the basicity of ligand backbone sites, but

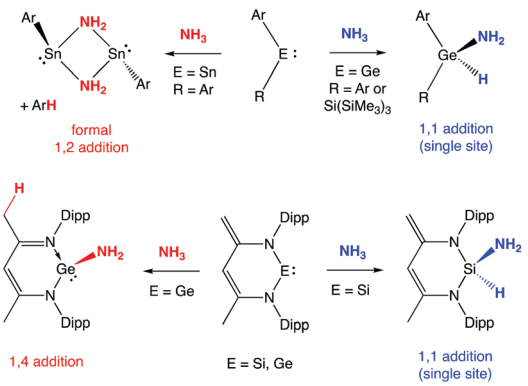

Scheme 1 Different modes of N–H activation previously reported for germylene and related systems (Ar = 2,6,-$C_6H_3Mes_2$; Mes = 2,4,6-$Me_3C_6H_2$; Dipp = 2,6-$^iPr_2C_6H_3$).[3b–e,i]

[a]*Department of Chemistry, University of Oxford, Inorganic Chemistry Laboratory, South Parks Road, Oxford, OX1 3QR, UK. E-mail: simon.aldridge@chem.ox.ac.uk*
[b]*Department of Chemistry, Nanoscience Center, University of Jyväskylä, P. O. Box 35, FI-40014 University of Jyväskylä, Finland*

†Electronic supplementary information (ESI) available: Additional synthetic and characterizing data, representative NMR spectra of new compounds, xyz file for DFT optimized structure; CIFs available from the CCDC, references 1952091–1952095, 1952097 and 2005217–2005219. For ESI and crystallographic data in CIF or other electronic format see DOI: 10.1039/d0dt01960g

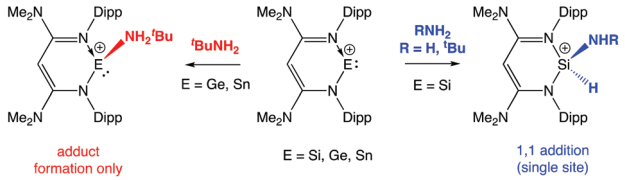

Scheme 2 N–H activation *vs.* amine coordination: reactions of N-nacnac stabilized silylium-, germylium- and stannylium-ylidenes with NH_3 and $^tBuNH_2$.[13]

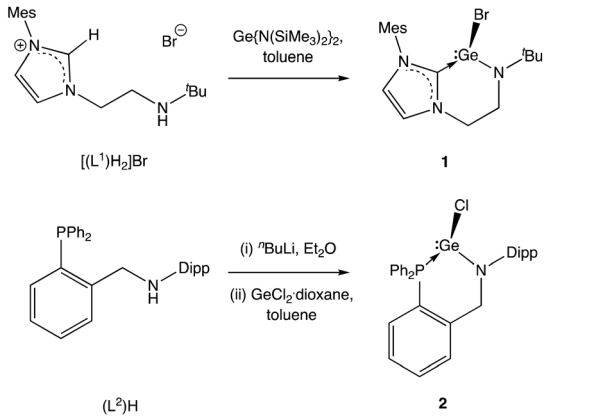

Scheme 3 Syntheses of halo-germylene precursors (L^1)GeBr (**1**) and (L^2)GeCl **2**.

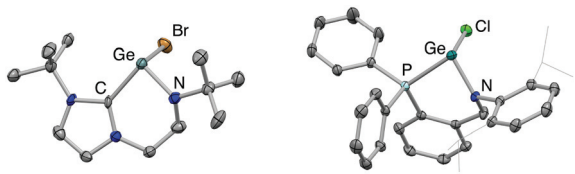

Fig. 1 Molecular structures of (L^1)GeBr (**1**, left) and (L^2)GeCl (**2**, right) as determined by X-ray crystallography. Thermal ellipsoids set at the 40% probability level and hydrogen atoms omitted for clarity. Key bond lengths (Å) and angles (°): (for **1**) Ge–C 2.07(1), Ge–N 1.866(9), Ge–Br 2.609(2), Br–Ge–C 94.3(3), Br–Ge–N 98.5(3), C–Ge–N 90.5(4); (for **2**) Ge–P 2.446(1), Ge–N 1.889(1), Ge–Cl 2.333(1), Cl–Ge–P 90.5(1), Cl–Ge–N 99.0(1), P–Ge–N 84.4(1).

also the ability of the donor set to promote formation of the Ge^{IV} oxidation state.[3b–f]

While charge-neutral tetrelenes of the type EX_2 have been investigated in some depth,[3] isoelectronic cations of the type $[R(L)E]^+$ have been less extensively studied,[7–12] despite the fact that the net positive charge should promote initial coordination of ammonia/amines, enhance the acidity of the NH bond and thereby promote N-to-E proton migration. We have recently examined the chemistry of N-nacnac supported tetrylium-ylidene cations towards N–H containing substrates, with the isolation of products derived from oxidative addition or simple amine adduct formation being found to be dependent on the group 14 element (Scheme 2).[13]

Given the lack of productivity in N–H activation exhibited by germylium-ylidene systems stabilized by these β-diketiminate (amido/imine) systems we were interested in (i) exploring the possibilities for the synthesis of two-coordinate amidogermylium-ylidene species stabilized by alternative (strong) donor sets (*e.g.* carbenes[14] and phosphines) which might promote the formation of Ge^{IV} products; and (ii) exploring the mode(s) of reactivity of such systems towards N–H bonds. These studies are reported in this manuscript.

Results and discussion

Germylium-ylidene synthesis

We initially targeted halo-germylene precursors featuring amido/NHC ligand $[L^1]^-$ or amido/phosphine ligand $[L^2]^-$ (Scheme 3). NHC-ligated bromo-germylene precursor **1** can be synthesized *via* one of two routes: (i) the reaction between protio-ligand $[(L^1)H_2]Br$ and one equivalent of the germanium (II) bis amide $Ge\{N(SiMe_3)_2\}_2$,[14,15] or (ii) *in situ* double deprotonation of $[(L^1)H_2]Br$ (*e.g.* with ^{n}BuLi) followed by metathesis with $GeCl_2$·dioxane. In our hands, route (i) is preferable, leading to yields of *ca.* 90%. By contrast, chloro-germylene complex **2** is most readily synthesized by deprotonation of (L^2)H, followed by reaction of the lithiated ligand with $GeCl_2$·dioxane. The overall yield for the two steps combined is typically in the region of 50%. Both **1** and **2** have been characterized by standard spectroscopic and analytical methods, and by X-ray crystallography (Fig. 1). The structures of both compounds in the solid state are in line with related complexes, featuring angles at the germanium centre which are close to 90° (*e.g.* 90.0(1)–98.9(1)° for **1**) consistent with the expected (low) degree of *ns*/*np* mixing for $n = 4$.[16]

From these precursors, two-coordinate NHC- or phosphine-stabilized Ge^{II} cations (germylium-ylidenes) can be synthesised by halide abstraction, most conveniently using $Li[Al(OC(CF_3)_3)_4]$ as a weakly coordinating anion (WCA) source (Scheme 4).[17] Treatment of **1** or **2** with $Li[Al(OC(CF_3)_3)_4]$ in bromobenzene at room temperature leads to the formation of the respective cationic species **3** and **4** in reasonable yields (30–40%).[18] In both cases, the ^{1}H and ^{13}C NMR spectra reveal distinct changes from the respective bromogermylene precursor: for **3** the N^{t}Bu signal is shifted from δ_H = 1.42 to 0.98 ppm, and the carbenic ^{13}C resonance is shifted upfield from δ_C = 169.5 to 165.6 ppm. In the case of phosphine-ligated system **4**, the ^{31}P resonance is shifted from δ_P = −24.4 (for **2**) to −2.2 ppm.

Both **3** and **4** could be obtained as single crystals suitable for X-ray diffraction, to allow for unambiguous confirmation of the monomeric two-coordinate structures in the solid state (Fig. 2). Cation formation is reflected in marked shortening of the Ge–N bonds compared to precursors **1** and **2**, presumably due to enhanced possibilities for N-to-Ge π bonding in the two-coordinate systems (*e.g.* *d*(Ge–N) = 1.889(1), 1.811(3) Å for **2** and **4**, respectively). Consistently, in both cases, the geometry

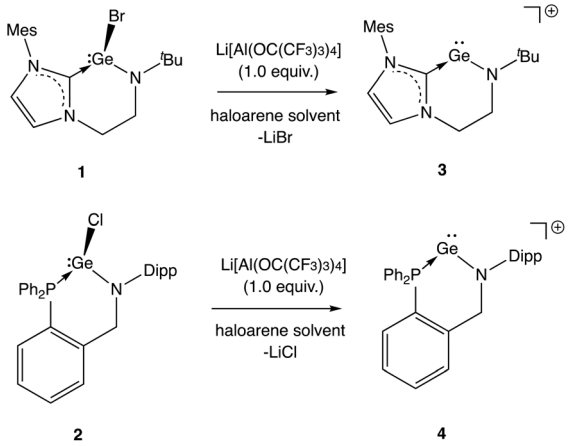

Scheme 4 Generation of cationic species *via* halide abstraction from **1** and **2** (anions omitted for clarity).

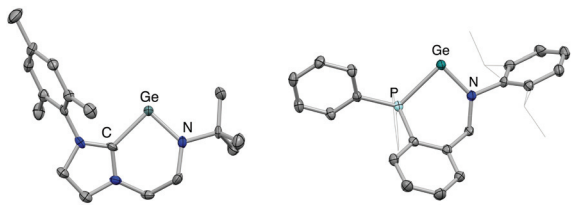

Fig. 2 Molecular structures of the cationic component of $[(L^1)Ge][Al(OC(CF_3)_3)_4]$ (**3**, left) and one of the cationic components in the asymmetric unit of $[(L^2)Ge][Al(OC(CF_3)_3)_4]$ (**4**, right) as determined by X-ray crystallography. Thermal ellipsoids set at the 40% probability level. Anions, second component of the asymmetric unit (for **4**) and hydrogen atoms omitted, and selected substituents shown in wireframe format for clarity. Key bond lengths (Å) and angles (°): (for **3**) Ge–N 1.829(4), Ge–C 2.040(4), C–Ge–N 91.9(2); (for **4**) Ge–N 1.811(3), Ge–P 2.449(1), P–Ge–N 88.5(1).

around the amido nitrogen is significantly more planar than in the halo-germylene precursor (*e.g.* 359.7° for **3** *vs.* 350.0° for **1**). The distances from germanium to the neutral NHC or phosphine donor, on the other hand, are much less affected by halide abstraction (*e.g.* *d*(Ge–P) = 2.446(1), 2.449(1) Å for **2** and **4**, respectively). In each cation, the angle subtended at germanium is relatively narrow (91.9(2) and 88.5(1)° for **3** and **4**, respectively) reflecting the constraints of the six-membered chelate ring.[12] The effect of the differing strengths of the neutral donor (*i.e.* NHC *vs.* phosphine) on the Ge–N moiety appear not to be statistically significant: the Ge–N bond lengths for **3** and **4** are 1.829(4) and 1.811(3) Å, respectively.

These studies also reveal that the product obtained is strongly dependent on the conditions employed. In the case of **3**, clean product formation requires the use of a haloarene solvent (fluoro- or bromobenzene), while the use of benzene leads to the formation of different products arising from incomplete halide abstraction.[14] If the reaction is carried out in benzene using 0.5 equiv. of $Li[Al(OC(CF_3)_3)_4]$ the bromide-bridged digermanium system $[\{(L^1)Ge\}_2(\mu\text{-Br})][Al(OC(CF_3)_3)_4]$ (**5**)

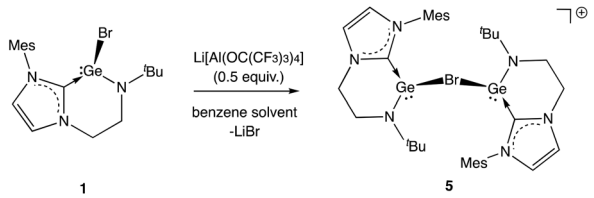

Scheme 5 Generation of monocationic digermanium species $[\{(L^1)Ge\}_2(\mu\text{-Br})][Al(OC(CF_3)_3)_4]$ (**5**) *via* incomplete halide abstraction from **1** in benzene solution (anion omitted for clarity).

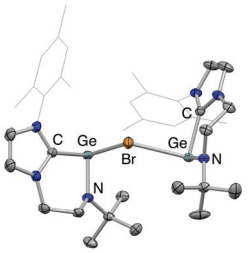

Fig. 3 Molecular structure of the cationic component of $[\{(L^1)Ge\}_2(\mu\text{-Br})][Al(OC(CF_3)_3)_4]$ (**5**) as determined by X-ray crystallography. Thermal ellipsoids set at the 40% probability level; anion and hydrogen atoms omitted and selected substituents shown in wireframe format for clarity. Key bond lengths (Å) and angles (°): Ge–N 1.857(1), 1.854(1), Ge–C 2.057(2), 2.062(2), Ge–Br 2.729(1), 2.768(1), Br–Ge–C 91.7(1), 88.6(1), Br–Ge–N 95.6(1), 97.9(1), C–Ge–N 90.2(1), 91.0(1).

is obtained, *via* trapping of the $[(L^1)Ge]^+$ cation by unreacted **1** (Scheme 5 and Fig. 3).

Reactivity studies – activation of N–H bonds

Mechanistically, the pathways for activation of E–H bonds by tetrelene and related systems are known to be dependent on the nature of E. For H_2, mechanisms have been advanced for carbene and silylene systems which involve simultaneous interaction of the substrate with the C/Si centred lone pair and the orthogonal, formally vacant, pπ orbital.[3a,19] The orientation of the H_2 molecule in the transition state then reflects the relative importance of the donor and acceptor capabilities of the tetrelene. Such mechanistic proposals emphasize the importance of the n-to-pπ energy gap (which is often equivalent to the HOMO–LUMO gap) in facilitating the activation of H_2.[20]

On the other hand, protic substrates, such as ammonia, have been shown to be activated by an alternative coordination/proton migration pathway.[3e,h,5,6,21] This sequence involves initial coordination of the NH_3 molecule, with the tetrelene acting as an electrophile. Subsequent N-to-E proton migration (facilitated, for example, by a second molecule of NH_3) then completes the formal N–H oxidative addition process.[3e,h,5,6] In this case it is the energy of the vacant pπ orbital of the tetrelene, and its consequent ability to coordinate and activate the NH_3 substrate that is thought to be important in bond cleavage.

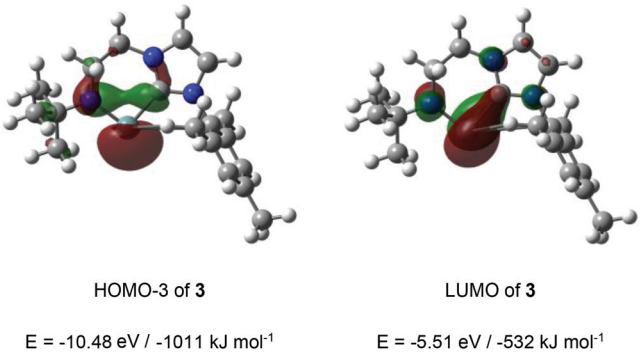

Fig. 4 Key germanium-centred frontier orbitals for the cationic component of **3**.

In the cases of cationic systems **3** and **4**, the presence of strongly π-donor amido α-substituents would be expected to lead to significant elevation of the Ge-centred pπ orbital, and this, taken together with the relative narrow angle at germanium in each case (and the associated high degree of 4*s* character in the lone pair) would be expected to lead to a wide *n*-to-pπ energy separation.[3i,22] Consistently, DFT calculations (PBE1PBE, Def2-TZVP level of theory), exemplified for **3** (Fig. 4) reveal that this separation is >400 kJ mol^{-1}. The LUMO features significant Ge pπ character, with some delocalization onto the carbene carbon, and the expected anti-bonding phase relationship with the N pπ orbital (Fig. 4). The germanium-centred lone pair is relatively low in energy, being associated with the HOMO−3.

Unsurprisingly then, we find that neither **3** and **4** shows any hint of reactivity towards H_2, or the hydridic E–H bonds present in $PhSiH_3$, Et_3SiH or $Me_3N{\cdot}BH_3$, for which more-or-less concerted oxidative activation would be expected. On the other hand, the low-lying nature of the orbital manifold (and the implied high Lewis acidity) for both systems would appear to be better suited to the activation of polar bonds, such as N–H linkages. Accordingly, the cleavage of N–H bonds can be demonstrated explicitly through the reactions of **3** and **4** with carbazole (Scheme 6). The corresponding reactions with ammonia are much more difficult to control in terms of stoichiometry,[23] and invariably result in the presence of protonated ligand among the products formed. Carbazole, by contrast, can easily be added stoichiometrically and its planar structure proves to be critical in isolating the reaction product by crystallization.

In contrast to two-coordinate diaryl germylene and cationic β-diketiminate silylium-ylidene complexes (Schemes 1 and 2), for which single-site N–H activation processes result in net oxidative addition at the group 14 element, the mode of activation in the cases of **3** and **4** involves 1,2-addition across the amido Ge–N bond (Scheme 6). As such, products **6** and **7** are generated, in which the Ge^{II} oxidation state is retained, the amido donor is protonated (to generate a secondary amine) and coordination of the anionic carbazolyl conjugate base increases the germanium coordination number from two to three.

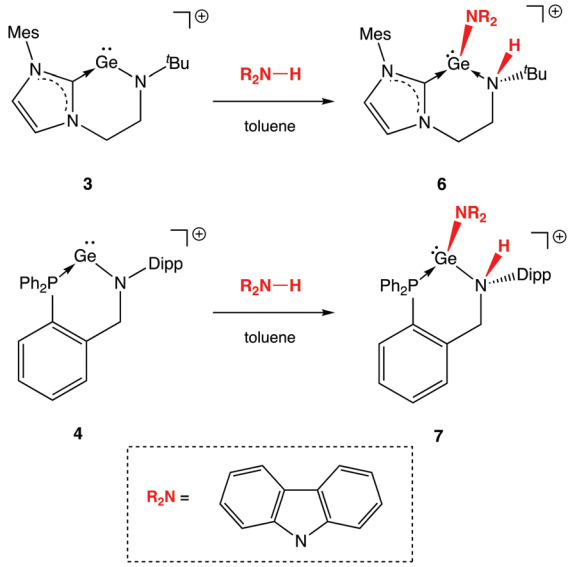

Scheme 6 Activation of N–H bonds in 1,2-fashion by NHC and phosphine stabilized germylium-ylidenes (anions omitted for clarity).

N–H bond formation is signalled in each case by the appearance of an additional signal in the respective ^{1}H NMR spectrum, at δ_H = 3.72 and 6.02 ppm (for **6** and **7**, respectively). In the case of **7**, the signal in question is a doublet with a $^3J_{HP}$ coupling of *ca.* 11 Hz to the germanium-bound phosphine donor. In addition (notwithstanding the problems associated with the definitive location of hydrogen atoms by X-ray crystallography), both the pyramidalization of the heavy atom skeleton at N and the lengthening of the Ge–N bond [1.829(4) to 2.134(7) Å for **3**/**6** and 1.811(3) to 2.137(4) Å for **4**/**7**] are also consistent with the conversion of an anionic amido donor to a charge neutral secondary amine ligand (Fig. 5). In addition, the location of the carbazolyl substituent and the H atom on the same face of the resulting cations **6** and **7** is consistent with a mechanistic hypothesis involving initial N-coordination

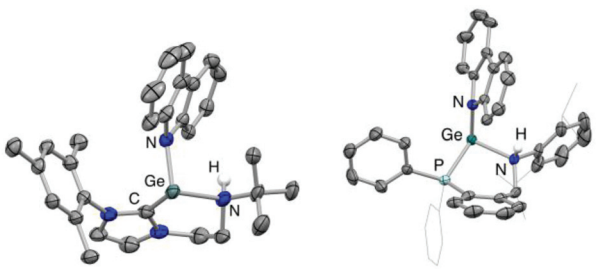

Fig. 5 Molecular structures of the cationic components of the N–H bond activation products $[(L^1H)Ge(NC_{12}H_8)][Al(OC(CF_3)_3)_4]$ (**6**, left) and $[(L^2H)Ge(NC_{12}H_8)][Al(OC(CF_3)_3)_4]$ (**7**, right), as determined by X-ray crystallo-graphy. Thermal ellipsoids set at the 40% probability level; cations and most hydrogen atoms omitted and selected substituents shown in wireframe format. Key bond lengths (Å) and angles (°): (for **6**) Ge–N 2.134(7), Ge–C 2.030(9), Ge–N_{carb} 1.935(7), C–Ge–N 87.5(3); (for **7**) Ge–N 2.137(4), Ge–P 2.481(1), Ge–N_{carb} 1.923(3), P–Ge–N 86.8(1).

at the highly Lewis acidic germanium centre followed by proton migration to the proximal amido ligand.[3e,h,5,6] Precedent for the formation of an initial donor/acceptor adduct of this sort comes from a recently reported β-diketiminate supported germylium-ylidene cation, which can be isolated due to the presence of a less acidic N–H bond and a less basic amido ligand.[13] Subsequent proton transfer to a basic ligand site has previously been reported for Nacnac-derived germanium and aluminium/gallium systems,[3d,g,24] and finds more general precedent in the pyridine-derived ligand systems pioneered by Milstein and co-workers.[25]

Conclusions

NHC- and phosphine-stabilized germylium-ylidene cations, featuring tethered amido substituents have been isolated for the first time and shown definitively to be two-coordinate in the solid state by X-ray crystallography. The presence of the strongly Lewis acidic cationic germanium centre and proximal amide function allows for facile cleavage of protic E–H bonds in cooperative (1,2-) fashion (exemplified by the N–H bond in carbazole), leading to the formation of a tethered secondary amine donor bound to a three-coordinate Ge^{II} centre. By analogy with chemistry reported for neutral stannylene and germylene systems,[3e,h,5,6] and consistent with structural results which imply that addition of the components of the E–H bond happen at *one face* of the Ge–N linkage, we propose that this chemistry proceeds *via* coordination of the substrate at the highly electrophilic germanium centre, followed by proton migration (*i.e.* intramolecular deprotonation) involving the nearby amide group. Such a sequence is consistent with the idea that substrate coordination *via* the pπ orbital at germanium markedly reduces the extent of N-to-Ge π donation from the amide, thereby enhancing the basicity of the proximal N-group. As such, the presence of the highly Lewis acidic site in cations of this sort is key to cooperative activation of the substrate across the germanium-nitrogen bond. Differences in the regiochemistry of N–H addition compared to other Ge^{II} systems (1,2- *vs.* 1,1- (single site) or 1,4-addition, for example),[3d,e] can then be rationalized on the basis of the location of the most accessible basic site within an initially formed amine adduct. Consistent with these hypotheses, we find that the HOMO of the model adduct **3**·NH_3 (at −9.18 eV/−886 kJ mol^{-1}) is characterized as the amide N lone pair: this orbital is elevated significantly from its counterpart in the free cation **3** (the HOMO-2 at −10.22 eV/−986 kJ mol^{-1}). The germanium-centred lone pair in the adduct **3**·NH_3 is found in the HOMO−1 (at −9.44 eV/−911 kJ mol^{-1}) (see ESI†).

Experimental

General considerations

All manipulations were carried out using standard Schlenk line or dry-box techniques under an atmosphere of argon. Toluene and hexane were degassed by sparging with argon and dried by passing through a column of the appropriate drying agent using a commercially available Braun SPS and stored over potassium; fluorobenzene and bromobenzene were dried by refluxing over CaH_2 and stored over molecular sieves. Benzene-d_6 was dried using a potassium mirror and bromobenzene-d_5 dried using CaH_2 and stored over molecular sieves. NMR samples were prepared under argon in 5 mm Wilmad 507-PP tubes fitted with J. Young Teflon valves. NMR spectra were measured on Bruker Avance III HD Nanobay or Bruker AVII spectrometers operating at 400 or 500 MHz, respectively (for ^{1}H measurements); ^{1}H and ^{13}C NMR spectra were referenced internally to residual protio-solvent (^{1}H) or solvent (^{13}C) resonances and are reported relative to tetramethylsilane. ^{19}F and ^{27}Al NMR spectra were referenced with respect to $CFCl_3$ and $[Al(H_2O)_6]^{3+}$, respectively. Chemical shifts are quoted in δ (ppm) and coupling constants in Hz. Elemental analyses were carried out at London Metropolitan University. Protio-ligands $[(L^1)H_2]Br$ and $(L^2)H$,[15] and metal precursors $Ge\{N(SiMe_3)_2\}_2$[26] and $Li[Al(OC(CF_3)_3)_4]$[17] were prepared *via* literature methods. $Li(L^2)$ was prepared from $(L^2)H$ and ^{n}BuLi as described in the ESI.†

DFT calculations

All computational work reported here was carried out using density functional theory (DFT) within the Gaussian16 (Revision C.01) program package.[27] Geometry optimizations were performed with the PBE1PBE exchange correlation functional,[28–30] using the Def2-TZVP basis set with an ultrafine integration grid and Grimme's empirical dispersion correction (GD3BJ).[31] The nature of stationary points found (minimum) was confirmed by full frequency calculations (no imaginary frequencies).

Crystallography

Single-crystal X-ray diffraction data for all compounds were collected using an Oxford Diffraction Supernova dual-source diffractometer equipped with a 135 mm Atlas CCD area detector. Crystals were selected under Paratone-N oil, mounted on MiTeGen Micromount loops and quench-cooled using an Oxford Cryosystems open flow N_2 cooling device.[32] Data were collected at 150 K using mirror monochromated Cu K_α radiation (λ = 1.5418 Å; Oxford Diffraction Supernova). Data collected were processed using the CrysAlisPro package, including unit cell parameter refinement and inter-frame scaling (which was carried out using SCALE3 ABSPACK within CrysAlisPro).[33] Equivalent reflections were merged and diffraction patterns processed with the CrysAlisPro suite.[33] Structure were solved *ab initio* from the integrated intensities using SHELXT[34] and refined on F^2 using SHELXL[34] with the graphical interface Olex2[35] or X-Seed.[36] Full details are given in the supplementary deposited CIF files (CCDC 1952091–1952095, 1952097 and 2005217–2005219†).

Syntheses of novel compounds

(L1)GeBr (1). To a mixture of $[(L^1)H_2]Br$ (600 mg, 1.64 mmol) and $Ge\{N(SiMe_3)_2\}_2$ (644 mg, 1.64 mmol) was added toluene

(15 mL) at −78 °C. The reaction mixture was warmed to room temperature and then heated to 80 °C for 2 d, over which time a colourless solution was formed. Volatiles were removed *in vacuo*, and **1** was isolated as a pale yellow powder. Single crystals suitable for X-ray crystallography were obtained from a concentrated solution in THF layered with hexane and stored at room temperature. Yield: 709 mg, 99%. ^{1}H NMR (400 MHz, benzene-d_6, 298 K): δ_H 1.42 (9H, s, ^{t}Bu), 2.00 (3H, s, *para* CH_3 of Mes), 2.06 (6H, br s, *ortho* CH_3 of Mes), 3.43 (4H, br s, CH_2), 5.89 (1H, br d, imidazolylidene backbone CH), 6.12 (1H, br d, imidazolylidene backbone CH), 6.68 (2H, s, CH of Mes). ^{13}C{^{1}H} NMR (126 MHz, benzene-d_6, 298 K): δ_C 18.5 (*ortho* CH_3 of Mes), 21.1 (*para* CH_3 of Mes), 30.7 (CH_3 of ^{t}Bu), 43.8 (quaternary C of ^{t}Bu), 52.5 (CH_2), 56.5 (CH_2), 121.3 (imidazolylidene backbone CH), 121.3 (imidazolylidene backbone CH), 128.4 (*para* C of Mes), 129.7 (*meta* CH of Mes), 133.0 (*ortho* C of Mes), 140.0 (*ipso* C of Mes), 169.5 (imidazolylidene C). Elemental microanalysis: calc. for $C_{18}H_{26}BrGeN_3$: C 49.48%, H 6.00%, N 9.62%; meas. C 49.54%, H 5.82%, N 9.53%. Crystallographic data: $C_{18}H_{26}BrGeN_3$, M_r = 436.92, orthorhombic, *Pbca*, a = 13.8454(3), b = 13.2083(3), c = 21.4808(7) Å, V = 13 928.28(18) Å^3, Z = 8, ρ_c = 1.478 g cm^{-3}, T = 150 K, λ = 1.54184 Å, R_1 = 0.0406 for 3229 observed unique reflections [$I > 2\sigma(I)$], wR_2 = 0.0983 for all 4070 unique reflections. Max. and min. residual electron densities 0.94, −0.43 e Å^{-3}. CCDC 1952092.†

(L2)GeCl (2). To a mixture of Li(L^2) (750 mg, 1.64 mmol) and $GeCl_2$·dioxane (379 mg, 1.64 mmol) was added toluene (15 mL) at −78 °C. The reaction mixture was warmed to room temperature and stirred for 12 h, over which time a light green suspension was formed. The reaction mixture was filtered, and the filtrate concentrated *in vacuo*. A small portion of hexane (1 mL) was added and the solution stored −30 °C to give **2** as a pale yellow crystalline solid. Single crystals suitable for X-ray crystallography were obtained from a concentrated solution in toluene layered with hexane and stored at −30 °C. Yield: 610 mg, 67%. ^{1}H NMR (400 MHz, benzene-d_6, 298 K): δ_H 1.01 (6H, br d, CH_3 of Dipp), 1.25 (6H, br, CH_3 of Dipp), 3.50 (2H, br sept, CH of Dipp), 4.76 (2H, br m, methylene CH_2), 6.66 (1H, br m, phenyl backbone CH), 6.84 (1H, br m, phenyl backbone CH), 6.89 (1H, br m, phenyl backbone CH), 6.95–7.15 (10H, m, aromatic H of PPh_2, phenyl CH and Dipp CH), 7.42 (4H, br m, PPh_2). ^{1}H NMR (400 MHz, toluene-d_8, 193 K): δ_H 0.46 (3H, d, $^3J_{HH}$ = 6.2 Hz, CH_3 of Dipp), 1.02 (3H, d, $^3J_{HH}$ = 6.2 Hz, CH_3 of Dipp), 1.40 (3H, d, $^3J_{HH}$ = 6.2 Hz, CH_3 of Dipp), 1.45 (3H, d, $^3J_{HH}$ = 6.2 Hz, CH_3 of Dipp), 2.79 (1H, q, $^3J_{HH}$ = 6.2 Hz, CH of Dipp), 3.35 (1H, d, $^2J_{HH}$ = 15.5 Hz, CH_2), 3.97 (1H, q, $^3J_{HH}$ = 6.2 Hz, CH of Dipp), 3.35 (1H, d, $^2J_{HH}$ = 15.5 Hz, methylene CH_2), 6.24 (1H, br m, phenyl backbone CH), 6.61 (1H, br m, phenyl backbone CH), 6.68 (1H, br m, phenyl backbone CH), 6.72–6.93 (10H, overlapping m, PPh_2, phenyl CH and Dipp CH), 7.06 (2H, br m, PPh_2), 7.28 (2H, br m, PPh_2). ^{13}C{^{1}H} NMR (126 MHz, benzene-d_6, 298 K): δ_C 24.6 (CH_3 of Dipp), 26.3 (CH_3 of Dipp), 28.9 (CH of Dipp), 59.8 (d, $^3J_{CP}$ = 10.6 Hz, methylene C), 124.0 (Dipp *para* C), 124.3 (Dipp *ortho* C), 124.3 (phenyl backbone C), 126.3 (Dipp *meta* C), 127.7 (d, $^3J_{CP}$ = 5.6 Hz, phenyl backbone C), 129.3 (d, $^2J_{CP}$ = 9.8 Hz, PPh_2), 129.6 (d, $^2J_{CP}$ = 8.9 Hz, phenyl backbone C), 131.3 (d, $^3J_{CP}$ = 2.0 Hz, PPh_2), 131.4 (d, $^4J_{CP}$ = 1.8 Hz, PPh_2), 134.4 (d, $^1J_{CP}$ = 10.3 Hz, PPh_2), 135.4 (d, $^4J_{CP}$ = 1.8 Hz, phenyl backbone C), 147.6 (d, $^2J_{CP}$ = 8.2 Hz, phenyl backbone C), 148.9 (d, $^1J_{CP}$ = 12.8 Hz, phenyl backbone C), 149.1 (Dipp *ipso* C). ^{31}P NMR (104 MHz, benzene-d_6, 298 K): δ_P −24.4 (s). Elemental microanalysis: calc. for $C_{31}H_{33}ClGeNP$: C 66.65%, H 5.95%, N 2.51%; meas. C 66.47%, H 5.75%, N 2.43%. Crystallographic data: $C_{31}H_{33}ClGeNP$, M_r = 558.67, triclinic, $P\bar{1}$, a = 9.1837(3), b = 11.0396(4), c = 14.5439(5) Å, α = 111.357(3)°, β = 90.475(3)°, γ = 90.475(3)°, V = 1371.34(9) Å^3, Z = 2, ρ_c = 1.353 g cm^{-3}, T = 150 K, μ(CuKα) = 3.105 mm^{-1}, λ = 1.54184 Å, R_1 = 0.0250 for 5273 observed unique reflections [$I > 2\sigma(I)$], wR_2 = 0.0672 for all 5691 unique reflections. Max. and min. residual electron densities 0.50, −0.25 e Å^{-3}. CCDC 2005217.†

[(L^1)Ge][Al(OC(CF_3)$_3$)$_4$] (3). To a suspension of Li[Al(OC(CF_3)$_3$)$_4$] (334 mg, 0.34 mmol) in bromobenzene (5 mL) was added a solution of compound **1** (150 mg, 0.34 mmol) at room temperature. The reaction mixture was stirred for 12 h, over which time a yellow solution and white precipitate were formed. Volatiles were removed *in vacuo* and compound **3** isolated as a yellow oil. Single crystals suitable for X-ray crystallography were obtained by a concentrated solution in bromobenzene layered with hexane stored at room temperature. Yield: 193 mg, 42%. ^{1}H NMR (400 MHz, bromobenzene-d_5, 298 K): δ_H 0.98 (9H, s, ^{t}Bu), 1.72 (6H, s, *ortho* CH_3 of Mes), 2.08 (3H, s, *para* CH_3 of Mes), 3.20 (2H, m, CH_2), 3.60 (2H, m, CH_2), 6.36 (1H, d, $^3J_{HH}$ = 1.7 Hz, imidazolylidene backbone CH), 6.55 (1H, d, $^3J_{HH}$ = 1.7 Hz, imidazolylidene backbone CH), 6.64 (2H, s, CH of Mes). ^{13}C{^{1}H} NMR (126 MHz, bromobenzene-d_5, 298 K): δ_C 17.5 (*ortho* CH_3 of Mes), 21.1 (*para* CH_3 of Mes), 30.4 (CH_3 of ^{t}Bu), 46.0 (CH_2), 51.5 (CH_2), 61.3 (quaternary C of ^{t}Bu), 79.5 (quaternary C of C(CF_3)$_3$), 121.9 (q, $^1J_{CF}$ = 294 Hz, CF_3 of C(CF_3)$_3$), 122.2 (imidazolylidene backbone CH), 122.7 (imidazolylidene backbone CH), 123.9 (*para* C of Mes), 130.1 (*meta* CH of Mes), 134.1 (*ortho* C of Mes), 141.7 (*ipso* C of Mes), 165.6 (imidazolylidene C). ^{19}F NMR (376 MHz, bromobenzene-d_5, 298 K): δ_F −74.6. ^{27}Al NMR (104 MHz, bromobenzene-d_5, 298 K): δ_{Al} 35.4. Crystallographic data: $C_{34}H_{26}AlF_{36}GeN_3O_4$, M_r = 1324.15, monoclinic, $P2_1/n$, a = 10.5246(1), b = 18.4838(3), c = 24.2497(3) Å, β = 98.747(1)°, V = 4662.54(11) Å^3, Z = 4, ρ_c = 1.886 g cm^{-3}, T = 150 K, λ = 1.54184 Å, R_1 = 0.0938, for 7840 observed unique reflections [$I > 2\sigma(I)$], wR_2 = 0.2713 for all 9656 unique reflections. Max. and min. residual electron densities 2.04, −1.52 e Å^{-3}. CCDC 1952094.†

[(L^2)Ge][Al(OC(CF_3)$_3$)$_4$] (4). To a mixture of (L^2)GeCl (200 mg, 0.36 mmol) and Li[Al(OC(CF_3)$_3$)$_4$] (474 mg, 0.36 mmol) was added bromobenzene (15 mL) at room temperature. The reaction mixture was stirred for 12 h, over which time a yellow solution and a white precipitate formed. The reaction mixture was filtered and volatiles removed *in vacuo* to obtain compound **4** as a yellow oil. Single crystals suitable for X-ray crystallography were obtained from a concentrated solution in bromobenzene layered with hexane and stored at −30 °C. Yield: 153 mg, 29%. ^{1}H NMR (400 MHz, bromobenzene-d_5, 298 K):

δ_H 0.81 (6H, d, $^3J_{HH}$ = 6.8 Hz, Dipp Me), 0.91 (6H, d, $^3J_{HH}$ = 6.8 Hz, Dipp Me), 2.30 (2H, sept, $^3J_{HH}$ = 6.8 Hz, Dipp CH), 4.17 (2H, br m, methylene CH_2), 6.91–6.99 (4H, overlapping m, phenyl backbone CH), 7.03–7.19 (10H, m, aromatic H of PPh_2), 7.28–7.36 (3H, overlapping m, Dipp *meta* and *para* CH). $^{13}C\{^1H\}$ NMR (126 MHz, bromobenzene-d_5, 298 K): δ_C 24.4 (CH_3 of Dipp), 25.9 (CH_3 of Dipp), 28.4 (Dipp CH), 65.1 (d, $^3J_{CP}$ = 13.4 Hz, methylene C), 79.9 ($C(CF_3)_3$), 121.9 (q, $^1J_{CF}$ = 292.7 Hz, $C(CF_3)_3$), 117.3 (d, $^1J_{CP}$ = 44.4 Hz, phenyl backbone C), 119.0 (d, $^1J_{CP}$ = 52.3 Hz, PPh_2), 125.1 (phenyl backbone C), 126.9 (phenyl backbone C), 130.1 (PPh_2), 130.4 (PPh_2), 130.7 (d, $^2J_{CP}$ = 11.6 Hz, phenyl backbone CH), 133.7 (d, $^2J_{CP}$ = 11.3 Hz, PPh_2), 134.0 (Dipp C), 134.2 (d, $^4J_{CP}$ = 2.6 Hz, phenyl backbone C), 134.5 (Dipp C), 141.6 (d, $^3J_{CP}$ = 11.1 Hz, phenyl backbone C), 142.6 (d, $^1J_{CP}$ = 27.7 Hz, Dipp C), 145.6 (Dipp *ipso* C). ^{19}F NMR (376 MHz, bromobenzene-d_5, 298 K): δ_F −74.9. ^{27}Al NMR (104 MHz, bromobenzene-d_5, 298 K): δ_{Al} 35.1. ^{31}P NMR (104 MHz, bromobenzene-d, 298 K): δ_P −2.15 (s). Elemental microanalysis: calc. for $C_{47}AlF_{36}O_4H_{33}BrGeNP$: C 37.88%, H 2.23%, N 0.94%; meas. C 37.87%, H 2.61%, N 0.90%. Crystallographic data: $C_{47}AlF_{36}O_4H_{33}BrGeNP$, M_r = 1490.28, triclinic, $P\bar{1}$, a = 12.1911(3), b = 15.3762(6), c = 29.9659(10) Å, α = 83.214(3)°, β = 88.694(2)°, γ = 87.381(2)°, V = 5571.2(3) Å^3, Z = 4, ρ_c = 1.777 g cm^{-3}, T = 150 K, μ(CuKα) = 2.718 mm^{-1}, λ = 1.54184 Å, R_1 = 0.0647 for 19 220 observed unique reflections [$I > 2\sigma(I)$], wR_2 = 0.1824 for all 24 700 unique reflections. Max. and min. residual electron densities 1.84, −0.86 e Å^{-3}. CCDC 2005219.†

[{(L^1)Ge}$_2$(μ-Br)][Al(OC(CF$_3$)$_3$)$_4$] (5). To a mixture of **1** (200 mg, 0.46 mmol) and Li[Al{OC(CF$_3$)$_3$}$_4$] (223 mg, 0.23 mmol) was added benzene (10 mL) at room temperature. The reaction mixture was stirred overnight, over which time a yellow solution and white precipitate were formed. Volatiles were removed *in vacuo* and compound **5** isolated as a yellow oil. Single crystals suitable for X-ray crystallography were obtained from a concentrated solution in dichloromethane layered with hexane and stored at −30 °C. Yield: 276 mg, 34%. ^1H NMR (400 MHz, benzene-d_6, 298 K): δ_H 1.09 (9H, s, ^{t}Bu), 1.78 (6H, s, *ortho* CH_3 of Mes), 2.11 (3H, s, *para* CH_3 of Mes), 3.19 (2H, m, CH_2), 3.33 (2H, m, CH_2), 5.84 (1H, d, $^3J_{HH}$ = 1.9 Hz, imidazolylidene backbone CH), 6.12 (1H, d, $^3J_{HH}$ = 1.9 Hz, imidazolylidene backbone CH), 6.67 (2H, s, CH of Mes). $^{13}C\{^1H\}$ NMR (126 MHz, benzene-d_6, 298 K): δ_C 17.9 (*ortho* CH_3 of Mes), 20.9 (*para* CH_3 of Mes), 30.3 (CH_3 of ^{t}Bu), 44.5 (CH_2), 51.6 (CH_2), 57.6 (quaternary C of ^{t}Bu), 86.7 (quaternary C of $C(CF_3)_3$), 121.9 (imidazolylidene backbone CH), 122.3 (q, $^1J_{CF}$ = 292.7 Hz, CF_3 of $C(CF_3)_3$), 122.5 (imidazolylidene backbone CH), 129.8 (*para* C of Mes), 132.4 (*meta* CH of Mes), 134.8 (*ortho* C of Mes), 140.5 (*ipso* C of Mes), 166.0 (imidazolylidene C). ^{19}F NMR (376 MHz, benzene-d_6, 298 K): δ_F −75.7. ^{27}Al NMR (104 MHz, benzene-d_6, 298 K): δ_{Al} 34.7. Elemental microanalysis: calc. for $C_{51}H_{49}AlBrF_{46}Ge_2N_6O_4$: C 35.08%, H 2.83%, N 4.81%; meas. C 35.19%, H 2.97%, N 4.46%. Crystallographic data: $C_{51}H_{49}AlBrF_{36}Ge_2N_6O_4$, M_r = 1761.06, triclinic, $P\bar{1}$, a = 11.0633(1), b = 18.7791(2), c = 18.8201 (2) Å, α = 61.968(1), β = 80.591(1), γ = 80.424(1)°, V = 3386.38(7) Å^3, Z = 2, ρ_c = 1.727 g cm^{-3}, T = 150 K, λ = 1.54184 Å, R_1 = 0.0265, for 13 008 observed unique reflections [$I > 2\sigma(I)$], wR_2 = 0.0681 for all 14 100 unique reflections. Max. and min. residual electron densities 0.66, −0.51 e Å^{-3}. CCDC 1952095.†

[(L^{1}H)Ge(NC$_{12}$H$_8$)][Al(OC(CF$_3$)$_3$)$_4$] (6). To a solution of **3** (generated *in situ* from **1** (200 mg, 0.46 mmol) and Li[Al(OC(CF$_3$)$_3$)$_4$] (446 mg, 0.46 mmol) in fluorobenzene (5 mL)) was added dropwise at room temperature a solution of carbazole (7.7 mg, 0.46 mmol) in fluorobenzene (3 mL), and the reaction mixture warmed to room temperature. After stirring for 12 h, the reaction mixture was filtered and volatiles removed *in vacuo* to obtain **6** as a white solid. Single crystals suitable for X-ray crystallography were obtained from a concentrated solution in fluorobenzene layered with hexane stored at room temperature. Yield: 410 mg, 60%. ^1H NMR (400 MHz, bromobenzene-d_5, 298 K): δ_H 0.33 (9H, s, ^{t}Bu), 0.69 (3H, s, *para* CH_3 of Mes), 1.83 (3H, s, *ortho* CH_3 of Mes), 1.87 (3H, s, *ortho* CH_3 of Mes), 2.83 (1H, br m, CH), 3.02 (1H, br m, CH_2), 3.72 (1H, m, NH), 3.98 (1H, br m, CH_2), 4.28 (1H, br m, CH_2), 5.80 (1H, s, CH of Mes), 6.46 (1H, d, $^3J_{HH}$ = 1.8 Hz, imidazolylidene backbone CH), 6.64 (1H, s, *meta* CH), 6.76 (1H, d, $^3J_{HH}$ = 1.8 Hz, imidazolylidene backbone CH), 7.08 (4H, overlapping m, carbazolyl), 7.88 (4H, overlapping m, carbazolyl). $^{13}C\{^1H\}$ NMR (126 MHz, bromobenzene-d_5, 298 K): δ_C 16.5 (*para* CH_3 of Mes), 17.8 (*ortho* CH_3 of Mes), 21.0 (*ortho* CH_3 of Mes), 25.4 (CH_3 of ^{t}Bu), 42.6 (CH_2), 48.2 (CH_2), 59.0 (quaternary C of ^{t}Bu), 78.4 (quaternary C of $C(CF_3)_3$), 119.7 (carbazolyl), 120.5 (carbazolyl), 120.6 (carbazolyl), 121.8 (q, $^1J_{CF}$ = 294 Hz, CF_3 of $C(CF_3)_3$), 122.7 (imidazolylidene backbone CH), 124.8 (imidazolylidene backbone CH), 126.0 (carbazolyl), 126.4 (carbazolyl), 126.4 (carbazolyl), 129.2 (*meta* CH of Mes), 129.3 (*meta* CH of Mes), 130.8 (*ortho* C of Mes), 133.2 (*ortho* C of Mes), 135.4 (*para* C of Mes), 141.5 (*ipso* C of Mes), 164.7 (imidazolylidene C). ^{19}F NMR (376 MHz, bromobenzene-d_5, 298 K): δ_F −74.6. ^{27}Al NMR (104 MHz, bromobenzene-d_5, 298 K): δ_{Al} 35.4. Elemental microanalysis: calc. for $C_{46}H_{35}AlF_{36}GeN_4O_4$: C 37.05%, H 2.37%, N 3.76%; meas. C 36.94%, H 2.55%, N 3.69%. Crystallographic data (for fluorobenzene hemisolvate): $C_{49}H_{37.5}AlF_{36.5}GeN_4O_4$ (M_r = 1539.40): orthorhombic, *Fdd*2, a = 80.2560(12), b = 29.4338(5), c = 10.7141(2) Å, V = 25 309.3(7) Å^3, Z = 16, ρ_c = 1.616 g cm^{-3}, T = 150 K, λ = 1.54184 Å, R_1 = 0.1155 for 12 751 observed unique reflections [$I > 2\sigma(I)$], wR_2 = 0.3316 for all 13 230 unique reflections. Max. and min. residual electron densities 0.63, −0.39 e Å^{-3}. CCDC 1952097.†

[(L^{2}H)Ge(NC$_{12}$H$_8$)][Al(OC(CF$_3$)$_3$)$_4$] (7). A solution of **4** (generated *in situ* from **2** (200 mg, 0.36 mmol) and Li[Al(OC(CF$_3$)$_3$)$_4$] (474 mg, 0.36 mmol) in fluorobenzene (15 mL)) was added to solid carbazole (60 mg, 0.36 mmol). On stirring at room temperature for 12 h, the colour of the reaction mixture changed from orange to yellow. Single crystals of **7** suitable for X-ray crystallography were obtained from a concentrated solution in fluorobenzene layered with hexane and stored at −30 °C. Yield: 387 mg, 43%. ^1H NMR (400 MHz, bromobenzene-d_5, 298 K): δ_H 0.03 (3H, d, $^3J_{HH}$ = 6.3 Hz, CH_3 of Dipp), 0.60 (3H, d, $^3J_{HH}$ = 6.8 Hz, CH_3 of Dipp), 0.65 (3H, d, $^3J_{HH}$ = 6.62 Hz, CH_3 of Dipp), 1.18 (3H, d, $^3J_{HH}$ = 6.6 Hz, CH_3 of Dipp), 2.41 (1H, sept,

$^3J_{HH}$ = 7.1 Hz, CH of Dipp), 2.43 (1H, sept, $^3J_{HH}$ = 6.5 Hz, CH of Dipp), 3.88 (1H, br m, methylene CH), 4.59 (1H, br m, methylene CH), 6.02 (1H, d, $^3J_{HP}$ = 11.1 Hz, NH), 6.55 (1H, dd, $^3J_{HH}$ = 6.6 Hz, $^4J_{HH}$ = 2.5 Hz, Dipp *meta* CH), 6.87–6.91 (2H, m, Dipp *meta*/*para* CH), 7.08–7.37 (13H, m, PPh_2 and phenyl backbone CH), 7.42–7.54 (8H, br m, carbazole aromatic H), 7.97 (1H, m, phenyl backbone CH). $^{13}C\{^1H\}$ NMR (126 MHz, bromobenzene-d_5, 298 K): δ_C 21.7 (CH_3 of Dipp), 23.5 (CH_3 of Dipp), 24.1 (CH_3 of Dipp), 24.3 (CH_3 of Dipp), 31.8 (2 overlapping signals, CH of Dipp), 58.3 (d, $^3J_{CP}$ = 6.3 Hz, methylene C), 79.9 ($C(CF_3)_3$), 110.9 (PPh_2), 119.7 (PPh_2), 120.5 (phenyl backbone CH), 121.6 (PPh_2), 121.8 (carbazolyl), 121.9 (q, $^1J_{CF}$ = 292.3 Hz, $C(CF_3)_3$), 123.6 (phenyl backbone CH), 124.2 (carbazolyl), 127.4 (Dipp C), 130.8 (Dipp C), 131.7 (carbazolyl), 133.5 (carbazolyl), 133.6 (phenyl backbone C), 133.7 (phenyl backbone C), 134.1 (carbazolyl), 134.5 (carbazolyl), 134.6 (phenyl backbone C), 134.8 (Dipp *ipso* C), 136.8 (d, $^1J_{CP}$ = 14.7 Hz, PPh_2), 139.6 (phenyl backbone C), 140.9 (Dipp *ortho* C). ^{19}F NMR (376 MHz, bromobenzene-d_5, 298 K): δ_F −74.9. ^{27}Al NMR (104 MHz, bromobenzene-d_5, 298 K): δ_{Al} 35.1. ^{31}P NMR (104 MHz, bromobenzene-d, 298 K): δ_P −9.4 (s). Crystallographic data: $C_{59}H_{42}F_{36}AlGeN_2O_4$, M_r = 1657.48, monoclinic, *C*2/*c*, *a* = 28.6853(7), *b* = 18.4131(3), *c* = 29.1049(8) Å, β = 120.236(4)°, *V* = 13 281.4(7) Å^3, *Z* = 8, ρ_c = 1.658 g cm^{-3}, *T* = 150 K, μ(CuKα) = 2.356 mm^{-1}, λ = 1.54184 Å, R_1 = 0.0669 for 10 222 observed unique reflections [$I > 2\sigma(I)$], wR_2 = 0.1958 for all 13 689 unique reflections. Max. and min. residual electron densities 0.737, −0.595 e Å^{-3}. CCDC 2005218.†

Conflicts of interest

There are no conflicts to declare.

Acknowledgements

We acknowledge funding from the Academy of Finland (project number 314794, PV), the Oxford-SCG Centre of Excellence and the Leverhulme Trust (grant number RP-2018-246, JH), the EPSRC (grant number EP/K014714/1, MAF) and the EU 7th Framework Program, Marie Skłodowska-Curie actions (grant number PIEF-GA-2013-626441 for an IEF Fellowship, EK). We also thank Oxford University Advanced Research Computing (ARC) facilities for computational resources.

Notes and references

1 See, for example; (*a*) J. Haggin, *Chem. Eng. News*, 1993, **71**, 23; (*b*) J. L. Klinkenberg and J. F. Hartwig, *Angew. Chem., Int. Ed.*, 2011, **50**, 86–95.

2 For examples of transition metal activation of NH_3 by a range of mechanisms: (*a*) E. G. Bryan, B. F. G. Johnson and J. Lewis, *J. Chem. Soc., Dalton Trans.*, 1977, 1328–1330; (*b*) G. L. Hillhouse and J. E. Bercaw, *J. Am. Chem. Soc.*, 1984, **106**, 5472–5478; (*c*) A. L. Casalnuovo, J. C. Calabrese and D. Milstein, *Inorg. Chem.*, 1987, **26**, 973–976; (*d*) M. M. Banaszak Holl, P. T. Wolczanski and G. D. Van Duyne, *J. Am. Chem. Soc.*, 1990, **112**, 7989–7994; (*e*) J. Zhao, A. S. Goldman and J. F. Hartwig, *Science*, 2005, **307**, 1080–1082; (*f*) Y. Nakajima, H. Kameo and H. Suzuki, *Angew. Chem., Int. Ed.*, 2006, **45**, 950–952; (*g*) C. M. Fafard, D. Adhikari, B. M. Foxman, D. J. Mindiola and O. V. Ozerov, *J. Am. Chem. Soc.*, 2007, **129**, 10318–10319; (*h*) E. Khaskin, M. A. Iron, L. J. W. Shimon, J. Zhang and D. Milstein, *J. Am. Chem. Soc.*, 2010, **132**, 8542–8543; (*i*) I. Mena, M. A. Casado, P. García-Orduña, V. Polo, F. J. Lahoz, A. Fazal and L. A. Oro, *Angew. Chem., Int. Ed.*, 2011, **50**, 11735–11738; (*j*) T. Kimura, N. Koiso, K. Ishiwata, S. Kuwata and T. Ikariya, *J. Am. Chem. Soc.*, 2011, **133**, 8880–8883; (*k*) D. V. Gutsulyak, W. E. Piers, J. Borau-Garcia and M. Parvez, *J. Am. Chem. Soc.*, 2013, **135**, 11776–11779; (*l*) Y.-H. Chang, Y. Nakajima, H. Tanaka, K. Yoshizawa and F. Ozawa, *J. Am. Chem. Soc.*, 2013, **135**, 11791–11794; (*m*) R. M. Brown, J. Borau Garcia, J. Valjus, C. J. Roberts, H. M. Tuononen, M. Parvez and R. Roesler, *Angew. Chem., Int. Ed.*, 2015, **54**, 6274–6277; (*n*) E. Despagnet-Ayoub, M. K. Takase, J. A. Labinger and J. E. Bercaw, *J. Am. Chem. Soc.*, 2015, **137**, 10500–10503; (*o*) M. J. Bezdek, S. Guo and P. Chirik, *Science*, 2016, **354**, 730–733; (*p*) G. Margulieux, M. J. Bezdek, Z. R. Turner and P. J. Chirik, *J. Am. Chem. Soc.*, 2017, **139**, 6110–6113; (*q*) E. A. LaPierre, W. E. Piers and C. Gendy, *Dalton Trans.*, 2018, **47**, 16789–16797.

3 For examples of NH_3 activation by carbenes and heavier group 14 analogues, see for example: (*a*) G. D. Frey, V. Lavallo, B. Donnadieu, W. W. Schoeller and G. Bertrand, *Science*, 2007, **316**, 439–441; (*b*) Y. Peng, B. D. Ellis, X. Wang and P. P. Power, *J. Am. Chem. Soc.*, 2008, **130**, 12268–12269; (*c*) A. Jana, C. Schulzke and H. W. Roesky, *J. Am. Chem. Soc.*, 2009, **131**, 4600–4601; (*d*) A. Jana, I. Objartel, H. W. Roesky and D. Stalke, *Inorg. Chem.*, 2009, **48**, 798–800; (*e*) Y. Peng, J.-D. Guo, B. D. Ellis, Z. Zhu, J. C. Fettinger, S. Nagase and P. P. Power, *J. Am. Chem. Soc.*, 2009, **131**, 16272–16282; (*f*) A. Meltzer, S. Inoue, C. Präsang and M. Driess, *J. Am. Chem. Soc.*, 2010, **132**, 3038–3046; (*g*) W. Wang, S. Inoue, S. Yao and M. Driess, *Organometallics*, 2011, **30**, 6490–6494; (*h*) A. V. Protchenko, J. I. Bates, L. M. A. Saleh, M. P. Blake, A. D. Schwarz, E. L. Kolychev, A. L. Thompson, C. Jones, P. Mountford and S. Aldridge, *J. Am. Chem. Soc.*, 2016, **138**, 4555–4564; (*i*) M. Usher, A. V. Protchenko, A. Rit, J. Campos, E. L. Kolychev, R. Tirfoin and S. Aldridge, *Chem. – Eur. J.*, 2016, **22**, 11685–11698; (*j*) D. Wendel, T. Szilvási, D. Henschel, P. J. Altmann, C. Jandl, S. Inoue and B. Rieger, *Angew. Chem., Int. Ed.*, 2018, **57**, 14575–14579. See also: (*k*) C. Präsang, M. Stoelzel, S. Inoue, A. Meltzer and M. Driess, *Angew. Chem., Int. Ed.*, 2010, **49**, 10002–10005.

4 For other examples of main group compounds capable of NH_3 activation see, for example: (*a*) Z. Zhu, X. Wang, Y. Peng, H. Lei, J. C. Fettinger, E. Rivard and P. P. Power,

Angew. Chem., Int. Ed., 2009, **48**, 2031–2034; (*b*) S. M. McCarthy, Y.-C. Lin, D. Devarajan, J. W. Chang, H. P. Yennawar, R. M. Rioux, D. H. Ess and A. T. Radosevich, *J. Am. Chem. Soc.*, 2014, **136**, 4640–4650; (*c*) T. Chu, I. Korobkov and G. I. Nikonov, *J. Am. Chem. Soc.*, 2014, **136**, 9195–9202; (*d*) J. Cui, Y. Li, R. Ganguly, A. Inthirarajah, H. Hirao and R. Kinjo, *J. Am. Chem. Soc.*, 2014, **136**, 16764–16767; (*e*) W. Zhao, S. M. McCarthy, T. Y. Lai, H. P. Yennawar and A. T. Radosevich, *J. Am. Chem. Soc.*, 2014, **136**, 17634–17644; (*f*) J. A. B. Abdalla, I. M. Riddlestone, R. Tirfoin and S. Aldridge, *Angew. Chem., Int. Ed.*, 2015, **54**, 5098–5102; (*g*) T. P. Robinson, D. M. De Rosa, S. Aldridge and J. M. Goicoechea, *Angew. Chem., Int. Ed.*, 2015, **54**, 13758–13763.

5 M. E. Alberto, N. Russo and E. Sicilia, *Chem. – Eur. J.*, 2013, **19**, 7835–7846.

6 For a related mode of coordination/activation of hydrazine see: Z. Brown, J.-D. Guo, S. Nagase and P. P. Power, *Organometallics*, 2012, **31**, 3768–3772.

7 For relevant reviews see: (*a*) M. Asay, C. Jones and M. Driess, *Chem. Rev.*, 2011, **111**, 354–396; (*b*) V. S. V. S. N. Swamy, S. Pal, S. Khan and S. S. Sen, *Dalton Trans.*, 2015, **44**, 12903–12923; (*c*) T. A. Engesser, M. R. Lichenthaler, M. Schleep and I. Krossing, *Chem. Soc. Rev.*, 2016, **45**, 789–899; (*d*) H. Fang, Z. Wang and X. Fu, *Coord. Chem. Rev.*, 2017, **344**, 214–237.

8 A quasi one-coordinate Ge^{II} cation: J. Li, C. Schenk, F. Winter, H. Scherer, N. Trapp, A. Higelin, S. Keller, R. Pöttgen, I. Krossing and C. Jones, *Angew. Chem., Int. Ed.*, 2012, **51**, 9557–9561.

9 Cyclopentadienyl supported Ge^{II} cations: (*a*) J. G. Winter, P. Portius, G. Kociok-Kohn, R. Steck and A. C. Filippou, *Organometallics*, 1998, **17**, 4176–4182 For a related example featuring neutral arene donor stabilization see, for example: (*b*) T. Probst, O. Steigelmann, J. Riede and H. Schmidbaur, *Angew. Chem., Int. Ed. Engl.*, 1990, **29**, 1397–1398.

10 N-Donor supported Ge^{II} cations: (*a*) H. V. R. Dias and Z. Wang, *J. Am. Chem. Soc.*, 1997, **119**, 4650–4655; (*b*) M. Stender, A. D. Phillips and P. P. Power, *Inorg. Chem.*, 2001, **40**, 5314–5315; (*c*) F. Cheng, J. M. Dyke, F. Ferrante, A. L. Hector, W. Levason, G. Reid, M. Webster and W. Zhang, *Dalton Trans.*, 2010, **39**, 847–856; (*d*) Y. Xiong, S. Yao, S. Inoue, A. Berkefeld and M. Driess, *Chem. Commun.*, 2012, **48**, 12198–12200.

11 Carbodiphosphorane-supported Ge^{II} cations: S. Khan, G. Gopakumar, W. Thiel and M. Alcarazo, *Angew. Chem., Int. Ed.*, 2013, **52**, 5644–5647.

12 Carbene-supported Ge^{II} cations: (*a*) P. A. Rupar, V. N. Staroverov, P. J. Ragogna and K. M. Baines, *J. Am. Chem. Soc.*, 2007, **129**, 15138–15139; (*b*) Y. Xiong, S. Yao, G. Tan, S. Inoue and M. Driess, *J. Am. Chem. Soc.*, 2013, **135**, 5004–5007; (*c*) K. Inomata, T. Watanabe and H. Tobita, *J. Am. Chem. Soc.*, 2014, **136**, 14341–14344; (*d*) K. Inomata, T. Watanabe, Y. Miyazaki and H. Tobita, *J. Am. Chem. Soc.*, 2015, **137**, 11935–11937; (*e*) A. Rit, R. Tirfoin and S. Aldridge, *Angew. Chem., Int. Ed.*, 2016, **55**, 378–382; (*f*) M. Roy, S. Fujimori, M. Ferguson, R. McDonald, N. Tokitoh and E. Rivard, *Chem. – Eur. J.*, 2018, **24**, 14392–14399; (*g*) R. J. Mangan, A. Rit, C. P. Sindlinger, R. Tirfoin, J. Campos, J. Hicks, K. E. Christensen, H. Niu and S. Aldridge, *Chem. – Eur. J.*, 2020, **26**, 306–315 See also: (*h*) A. Rit, J. Campos, H. Niu and S. Aldridge, *Nat. Chem.*, 2016, **8**, 1022–1026.

13 D. C. H. Do, A. V. Protchenko, M. Á. Fuentes, J. Hicks, P. Vasko and S. Aldridge, *Chem. Commun.*, 2020, **56**, 4684–4687.

14 Hahn and Glorius have reported attempts to synthesize germylium-ylidene systems featuring amido substituents and stabiliized by NHC donors, although no structural or reactivity data was reported: D. Paul, F. Heins, S. Krupski, A. Hepp, C. G. Daniliuc, K. Klahr, J. Neugebauer, F. Glorius and F. E. Hahn, *Organometallics*, 2017, **36**, 1001–1008.

15 (*a*) P. L. Arnold, S. A. Mungur, A. J. Blake and C. Wilson, *Angew. Chem., Int. Ed.*, 2003, **42**, 5981–5984; (*b*) B. Liu, D. Cui, J. Ma, X. Chen and X. Jing, *Chem. – Eur. J.*, 2007, **13**, 834–845.

16 M. Kaupp, in *The Chemical Bond: Fundamental Aspects of Chemical Bonding*, eds. G. Frenking and S. Shaik, Wiley-VCH, Weinheim, 2014, pp. 1–24.

17 I. Krossing, *Chem. – Eur. J.*, 2001, **7**, 490–502.

18 Similar chemistry can be used to access compounds analogous to **1** and **3** featuring an imidazole bound ^{t}Bu group (see ESI†).

19 (*a*) A. V. Protchenko, K. H. Birjkumar, D. Dange, A. D. Schwarz, D. Vidovic, C. Jones, N. Kaltsoyannis, P. Mountford and S. Aldridge, *J. Am. Chem. Soc.*, 2012, **134**, 6500–6503; (*b*) A. V. Protchenko, A. D. Schwarz, M. P. Blake, C. Jones, N. Kaltsoyannis, P. Mountford and S. Aldridge, *Angew. Chem., Int. Ed.*, 2013, **52**, 568–571.

20 P. P. Power, *Nature*, 2010, **463**, 171–177.

21 For key papers on the activation of related E–H bonds by germylenes, see, for example ref. 3*f*, and (*a*) J. W. Dube, Z. D. Brown, C. A. Caputo, P. P. Power and P. J. Ragogna, *Chem. Commun.*, 2014, **50**, 1944–1946; (*b*) Z. D. Brown, J. D. Erickson, J. C. Fettinger and P. P. Power, *Organometallics*, 2013, **32**, 617–622; (*c*) M. M. Juckel, J. Hicks, D. Jiang, L. Zhao, G. Frenking and C. Jones, *Chem. Commun.*, 2017, **53**, 12692–12695; (*d*) F. Diab, F. S. W. Aicher, C. P. Sindlinger, K. Eichele, H. Schubert and L. Wesemann, *Chem. – Eur. J.*, 2019, **25**, 4426–4434.

22 D. Bourissou, O. Guerret, F. P. Gabbaï and G. Bertrand, *Chem. Rev.*, 2000, **100**, 39–91.

23 Attempts to use thf solutions of ammonia invariably led to problems stemming from the strongly Lewis acidic nature of **3**/**4**.

24 J. A. B. Abdalla, I. M. Riddlestone, R. Tirfoin and S. Aldridge, *Angew. Chem., Int. Ed.*, 2015, **54**, 5098–5102.

25 (*a*) C. Gunanathan and D. Milstein, *Acc. Chem. Res.*, 2011, **44**, 588–602; (*b*) C. Gunanathan and D. Milstein, *Chem. Rev.*, 2014, **114**, 12024–12087.

26 D. H. Harris and M. F. Lappert, *J. Chem. Soc., Chem. Commun.*, 1974, 895–896.
27 M. J. Frisch, G. W. Trucks, H. B. Schlegel, G. E. Scuseria, M. A. Robb, J. R. Cheeseman, G. Scalmani, V. Barone, G. A. Petersson, H. Nakatsuji, X. Li, M. Caricato, A. V. Marenich, J. Bloino, B. G. Janesko, R. Gomperts, B. Mennucci, H. P. Hratchian, J. V. Ortiz, A. F. Izmaylov, J. L. Sonnenberg, D. Williams-Young, F. Ding, F. Lipparini, F. Egidi, J. Goings, B. Peng, A. Petrone, T. Henderson, D. Ranasinghe, V. G. Zakrzewski, J. Gao, N. Rega, G. Zheng, W. Liang, M. Hada, M. Ehara, K. Toyota, R. Fukuda, J. Hasegawa, M. Ishida, T. Nakajima, Y. Honda, O. Kitao, H. Nakai, T. Vreven, K. Throssell, J. A. Montgomery Jr., J. E. Peralta, F. Ogliaro, M. J. Bearpark, J. J. Heyd, E. N. Brothers, K. N. Kudin, V. N. Staroverov, T. A. Keith, R. Kobayashi, J. Normand, K. Raghavachari, A. P. Rendell, J. C. Burant, S. S. Iyengar, J. Tomasi, M. Cossi, J. M. Millam, M. Klene, C. Adamo, R. Cammi, J. W. Ochterski, R. L. Martin, K. Morokuma, O. Farkas, J. B. Foresman and D. J. Fox, *Gaussian 16, Revision C.01*, Gaussian, Inc., Wallingford CT, 2019.
28 J. P. Perdew, K. Burke and M. Ernzerhof, *Phys. Rev. Lett.*, 1996, **77**, 3865–3868.
29 J. P. Perdew, M. Ernzerhof and K. Burke, *J. Chem. Phys.*, 1996, **105**, 9982.
30 C. Adamo and V. Barone, *J. Chem. Phys.*, 1999, **110**, 6158–6170.
31 (*a*) F. Weigend and R. Ahlrichs, *Phys. Chem. Chem. Phys.*, 2005, **7**, 3297–3305; (*b*) F. Weigend, *Phys. Chem. Chem. Phys.*, 2006, **8**, 1057–1065; (*c*) S. Grimme, S. Ehrlich and L. Goerigk, *J. Comput. Chem.*, 2011, **32**, 1456–1465.
32 J. Cosier and A. M. Glazer, *J. Appl. Crystallogr.*, 1986, **19**, 105–107.
33 *CrysAlisPro, Agilent Technologies, Version 1.171.35.8*.
34 G. M. Sheldrick, *Acta Crystallogr., Sect. A: Found. Adv.*, 2015, **A71**, 3–8.
35 O. V. Dolomanov, L. J. Bourhis, R. J. Gildea, J. A. K. Howard and H. Puschmann, *J. Appl. Crystallogr.*, 2009, **42**, 339–341.
36 L. J. Barbour, *J. Supramol. Chem.*, 2001, **1**, 189–191.